

## Generation of chaotic dynamics by feedback on a laser

F. T. Arecchi,\* W. Gadomski,<sup>†</sup> and R. Meucci<sup>‡</sup>

*Istituto Nazionale di Ottica, I-50125 Firenze, Italy*

(Received 13 January 1986)

Self-pulsing and deterministic chaos is observed in a single-mode, homogeneous-line, CO<sub>2</sub> laser with an overall negative feedback, when the damping constant of the feedback loop is of the same order as the population decay rate. This represents a fundamental limitation of the general use of feedback schemes in high-stability laser applications. A theoretical model is shown to yield results in good agreement with the experimental ones, thus confirming the simple structure of the associated phase space.

In laser applications where high stability is required, an overall negative feedback is currently used, which is in addition to that already provided by the electromagnetic cavity, for instance, by controlling the pump strength with a signal provided by the detected output intensity.<sup>1</sup> Such a feedback is not just an added artifact, but affects in a fundamental way the dynamics of photon generation; indeed it has been proposed<sup>2</sup> as a means to provide squeezed states of the electromagnetic field, and preliminary evidence of such an effect has been given.<sup>3</sup> However, a fundamental objection to a feedback scheme is that it provides one extra dimension to phase space, and hence the modified dynamics can be affected by irregular behavior.

Here we report observation of self-pulsing and deterministic chaos in a single-mode laser fed back by its own output, that is, with the cavity losses modulated by a signal proportional to the output intensity. We further support the experimental evidence by a theoretical model which displays the dynamic features of a feedback laser. Notice that chaos due to feedback has already been observed in connection with nonlinear passive systems [either a potassium dihydrogen phosphate (KDP) crystal between crossed polarizers<sup>4</sup> or a long optical fiber in a ring cavity].<sup>5</sup> In both cases the passive system was studied *per se*, being outside the laser cavity, and thus the laser dynamics was not affected by the feedback configuration.

We have shown recently the onset of chaos in low-dimensional optical systems, in controlled conditions displaying a one-to-one correspondence between the outcomes of the experiment and those of the theoretical model. For this purpose, instead of pursuing a strict analogy with the Lorenz model<sup>6</sup> whose physical realization is only recent and still rather qualitative,<sup>7</sup> we have studied the so-called class *B* lasers,<sup>8</sup> that is, single-mode homogeneous-line lasers, where adiabatic elimination of the fast polarization variable reduces the dynamics to two coupled degrees of freedom (field amplitude and population inversion). A third degree of freedom, crucial for the onset of deterministic chaos, was provided in several ways: (i) by a nonautonomous driving applying a sinusoidal forcing to an intracavity modulator which modulates the cavity losses<sup>9,10</sup> or the cavity length,<sup>11</sup> (ii) by injection of field from an external detuned laser,<sup>8</sup> (iii) by a ring configuration, which decouples forward and backward waves, thus contributing at least one more degree of freedom<sup>12</sup> (in fact, as shown in Ref. 12 this latter system is modeled by seven coupled equations because of the nonlinear population grating induced by the two counterrunning waves). Purposefully, we did not tackle the vast class of inhomogeneously broadened lasers, where it is extremely difficult to drive close correspondences between experiments<sup>13</sup> and theory<sup>14</sup> because of the large number of coupled degrees of freedom.

Here we show a new way of introducing a third degree of freedom leading to chaotic instability, namely, feeding the laser output back on an intracavity modulator. When the feedback loop is so fast that it practically provides an "instantaneously" adapted loss coefficient, it does not modify the phase space topology, which in the case of a class *B* laser remains two dimensional. If, however, the time scale of the feedback loop is of the same order as that of the other relevant variables, the system becomes three dimensional. Let us refer to the experimental setup of Fig. 1. Such a system is ruled by three first-order equations for the intensity  $x$ , population difference  $y$ , and modulation voltage  $z$ . With suitable normalizations (we refer, e.g., to Ref. 9 for the unnormalized equations) the equations are

$$\begin{aligned}\dot{x} &= -k_0x(1 + a\sin^2z - y), \\ \dot{y} &= -\gamma(y - A + xy), \\ \dot{z} &= -\beta(z - B + fx),\end{aligned}\quad (1)$$

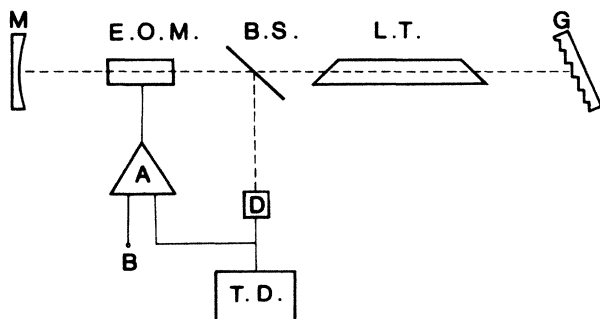


FIG. 1. Experimental setup with a CO<sub>2</sub> laser. M—total reflecting mirror mounted on a Piezo drive to control the mode tuning with respect to the center line, E.O.M.—electro-optic modulator, B.S.—beam splitter, L.T.—CO<sub>2</sub> laser tube, G—grating, A—high-voltage amplifier, D—HgCdTe detector, T.D.—transient digitizer, B—bias voltage.

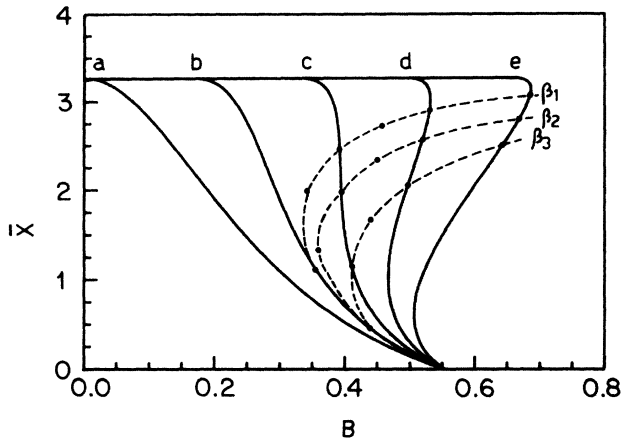


FIG. 2. Plots of normalized stationary intensity  $\bar{x}$  vs  $B$  (the bias-voltage  $B$  is expressed in angular units) for different values of the feedback coupling constant  $f$ . The curves a, b, c, d, and e refer to  $f=0$  (no feedback),  $f=0.052$ ,  $0.102$ ,  $0.152$ , and  $0.202$ , respectively. Dashed lines correspond to the loci of the first Hopf bifurcations for three different values of the damping constant ( $\text{sec}^{-1}$ ) of the feedback loop, namely,  $\beta_1=3.5 \times 10^4$ ,  $\beta_2=3.0 \times 10^4$ , and  $\beta_3=2.5 \times 10^4$ .

TABLE I. Values (kHz) of the first Hopf bifurcation.

$10^{-4}\beta$	$f=0.052$	$f=0.102$	$f=0.152$	$f=0.202$
2.5	...	31	39	57
3.0	45	16	39	49
3.5	51	15	29	36

where  $k(z) = k_0(1 + \alpha \sin^2 z)$  is the loss rate modulated by the voltage  $z$ ,  $k_0$  is the nonmodulated cavity loss parameter,  $\alpha = R/T$  is the ratio between reflection ( $R$ ) and transmission ( $T$ ) coefficient of the beam splitter corrected for the diffraction losses of the other optical elements within the cavity,  $\gamma$  is the population decay rate, and  $\beta$  the damping constant of the feedback loop. Furthermore,  $B$  is the voltage bias applied to the second input of the modulator amplifier,  $A$  is the pump parameter, and  $f$  is a coupling coefficient between intensity  $x$  detected on  $D$  and voltage  $z$ . Notice that  $x$  is normalized to the saturation intensity,  $y$  and  $A$  to the threshold population (without feedback), and  $z$  is given in angular units, that is, if we call  $v$  the voltage applied to the modulator and  $V$  the  $\lambda/2$  modulator

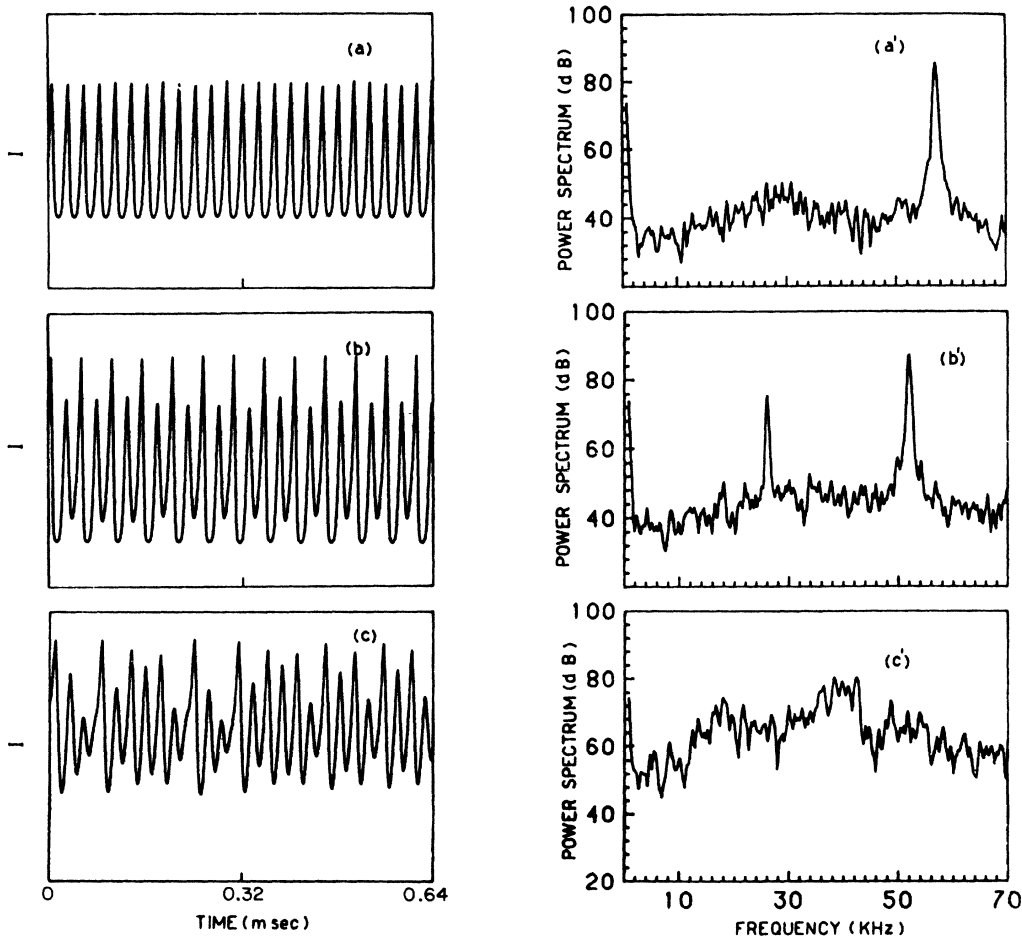


FIG. 3. Digitizer time plots of the experimental laser intensity (left side) and the corresponding power spectra (right-hand side) for increasing values of the control parameter  $B$ . (a) corresponds to the onset of the first Hopf bifurcation, at a frequency  $\nu=57.3$  kHz,  $B=0.364$ ; (b) shows the appearance of a subharmonic bifurcation  $f/2$  where the fundamental frequency is  $\nu=52.0$  kHz,  $B=0.378$ ; and (c) shows the appearance of chaos,  $B=0.383$ .

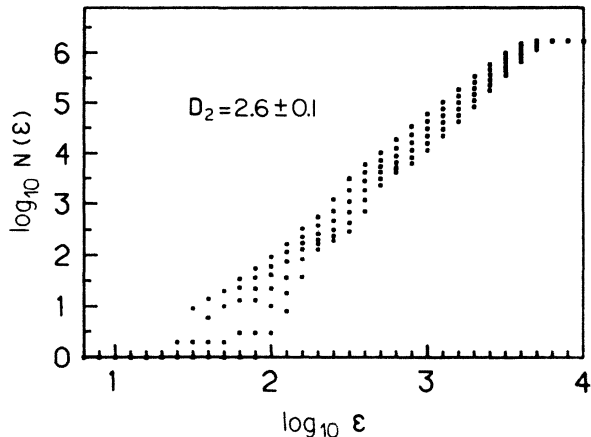


FIG. 4. Plots of  $\log_{10} N_n(\epsilon)$  vs  $\log_{10} \epsilon$  for different values of embedding dimension  $n$  ( $n=10-15$ ). Square dots come from experiment. Numerical solution of Eqs. (1) provides theoretical plots coinciding with the experimental ones within the dot sizes.

voltage, then  $z = \pi v/V$ .

In our experimental system we have chosen  $k_0 = 1.17 \times 10^7 (\text{sec}^{-1})$ ,  $\gamma = 0.98 \times 10^4 (\text{sec}^{-1})$ ,  $\beta = 3.0 \times 10^4 (\text{sec}^{-1})$ , and a normalized pump  $A = 4.2$ . The stationary solutions  $(\bar{x}, \bar{y}, \bar{z})$  of Eqs. (1) imply the condition

$$B = f\bar{x} + \arcsin \left[ \frac{A/\alpha}{1+\bar{x}} - \frac{1}{\alpha} \right]^{1/2}. \quad (2)$$

Depending on the feedback coupling  $f$ , for different bias values  $B$  we can have mono- or bistability (Fig. 2). In particular, around  $f=0.1$  we expect an ambiguity since Eq. (2) provides a quasivertical curve. Indeed, as we show later, this is the region where we observe chaos.

By a linear stability analysis around the stationary solution, we evaluate the points where the system starts self-pulsing (Hopf bifurcations). The lines of Hopf bifurcations are drawn in Fig. 2 (dashed) for three different  $\beta$  values. In fact, we have a slight uncertainty in the assignment of the open loop damping constant in our setup. At the intersection points of our stationary solutions (lines with fixed  $f$ ) with the lines of onset of Hopf bifurcations (lines with fixed  $\beta$ ) the corresponding pulsing frequency in kHz is given in Table I.

In Fig. 3 we present the power spectra of the intensity detected in our experiment. Figure 3(a) shows the first Hopf bifurcation, Fig. 3(b) the appearance of a subharmonic  $f/2$ , and Fig. 3(c) corresponds to the appearance of chaos. Beyond chaos, we observe periodic time windows. In order to get full assurance of the chaotic nature of the

TABLE II. Bifurcation parameters and Feigenbaum ratio.

Bifurcation	$B$	$\delta$
$f$	0.394 907	
$f/2$	0.395 355	
$f/4$	0.395 662	5.11
$f/8$	0.395 722	5.00
chaos	0.395 734	

time plot of 3(c), we have measured the Grassberger-Procaccia<sup>15</sup> or correlation dimension along the lines already outlined in Ref. 8.

Figure 4 shows clear evidence of a fractal exponent  $D_2 = 2.6 \pm 0.1$ . While Fig. 4 comes from the experiment, the same  $D_2$  value is obtained by solving numerically Eqs. (1) for  $\beta = \beta_2 = 3.0 \times 10^4$  and  $B = 0.383$ . The theoretical plots, when reported in Fig. 4, closely follow the experimental ones with uncertainties smaller than the dot sizes. Similar good agreement with the plots of Fig. 3 is obtained as we change  $B$  in Eqs. (1) according to the values given in the caption of Fig. 3. Experimentally, we have observed narrow regions with higher-order subharmonics ( $f/4$  and  $f/8$ ) plus  $f/3$  windows beyond chaos. In order to have a better understanding of the chaotic scenario, we have solved numerically Eqs. (1). An accurate localization of the bifurcation points was done by studying the stability of the phase space orbits in terms of their Floquet multipliers. More specifically, the multipliers were evaluated by determining the Poincaré sections with the Henon method,<sup>16</sup> and finding the zero of the associated recursive relation by the Newton method. In Table II we give the bifurcation diagram, which shows clear evidence of a Feigenbaum scenario with a Feigenbaum converging ratio in fair agreement with the asymptotic value.

In conclusion, we have shown theoretically and experimentally that the introduction of negative feedback provides a third dynamical degree of freedom sufficient to yield self-pulsing and chaotic behavior when the damping constant  $\beta$  of the feedback loop is of the same order as the population decay rate. As  $\beta$  is moved far away from this range of values, we expect the possibility of adiabatic elimination of one of the three variables of Eq. (1), and hence the cutoff of chaotic regimes. Such a further investigation is actually under way.

This work was supported in part by the Contract No. STI-082-J-C(CD) of the European Economic Community. We thank S. Cecchi, G. Giusfredi, A. Politi, and P. Salieri for helpful discussions.

\*Also with the Physics Department, University of Firenze, Italy.

†Permanent address: Department of Chemistry, Warsaw University, Warsaw, Poland.

‡Permanent address: Istituto di Cibernetica del C.N.R., I-80072 Arco Felice, Napoli, Italy.

§See, e.g., Instruction Manuals of current Argon or Krypton lasers commercially supplied by Coherent or Spectra Physics.

<sup>2</sup>H. A. Haus and Y. Yamamoto, in Proceedings of the MIT Workshop on Squeezed States of Light, Cambridge, October 21, 1985, edited by J. H. Shapiro and P. Kumar (unpublished).

<sup>3</sup>S. Machida and Y. Yamamoto, Opt. Commun. **57**, 290 (1986).

<sup>4</sup>F. A. Hopf, B. L. Kaplan, H. M. Gibbs, and R. L. Shoemaker, Phys. Rev. A **25**, 2172 (1982).

- <sup>5</sup>H. Nakatsuka, S. Asaka, H. Itoh, K. Ikeda, and M. Matsuoka, *Phys. Rev. Lett.* **50**, 109 (1983).
- <sup>6</sup>H. Haken, *Phys. Lett.* **53A**, 77 (1975).
- <sup>7</sup>E. H. M. Hogenboom, W. Klische, C. O. Weiss, and A. Godone, *Phys. Rev. Lett.* **55**, 2571 (1985).
- <sup>8</sup>F. T. Arecchi, G. L. Lippi, G. P. Puccioni, and J. R. Tredicce, *Opt. Commun.* **51**, 308 (1984).
- <sup>9</sup>F. T. Arecchi, R. Meucci, G. P. Puccioni, and J. R. Tredicce, *Phys. Rev. Lett.* **49**, 1217 (1982).
- <sup>10</sup>G. P. Puccioni, A. Poggi, W. Gadomski, J. R. Tredicce, and F. T. Arecchi, *Phys. Rev. Lett.* **55**, 339 (1985).
- <sup>11</sup>T. Midavaine, D. Dangoisse, and P. Glorieux, *Phys. Rev. Lett.* **55**, 1989 (1985).
- <sup>12</sup>G. L. Lippi, J. R. Tredicce, N. B. Abraham, and F. T. Arecchi, *Opt. Commun.* **53**, 129 (1985).
- <sup>13</sup>L. M. Hoffer, T. H. Chyba, and N. B. Abraham, *J. Opt. Soc. Am. B* **2**, 102 (1985).
- <sup>14</sup>L. W. Casperson, *J. Opt. Soc. Am. B* **2**, 62 (1985).
- <sup>15</sup>P. Grassberger and I. Procaccia, *Phys. Rev. Lett.* **50**, 346 (1983).
- <sup>16</sup>G. L. Oppo, A. Politi, G. L. Lippi, and F. T. Arecchi (unpublished).